Lab on a Chip

Miniaturisation for chemistry, physics, biology, materials science and bioengineering

www.rsc.org/loc

Volume 12 | Number 7 | 7 April 2012 | Pages 1193–1396

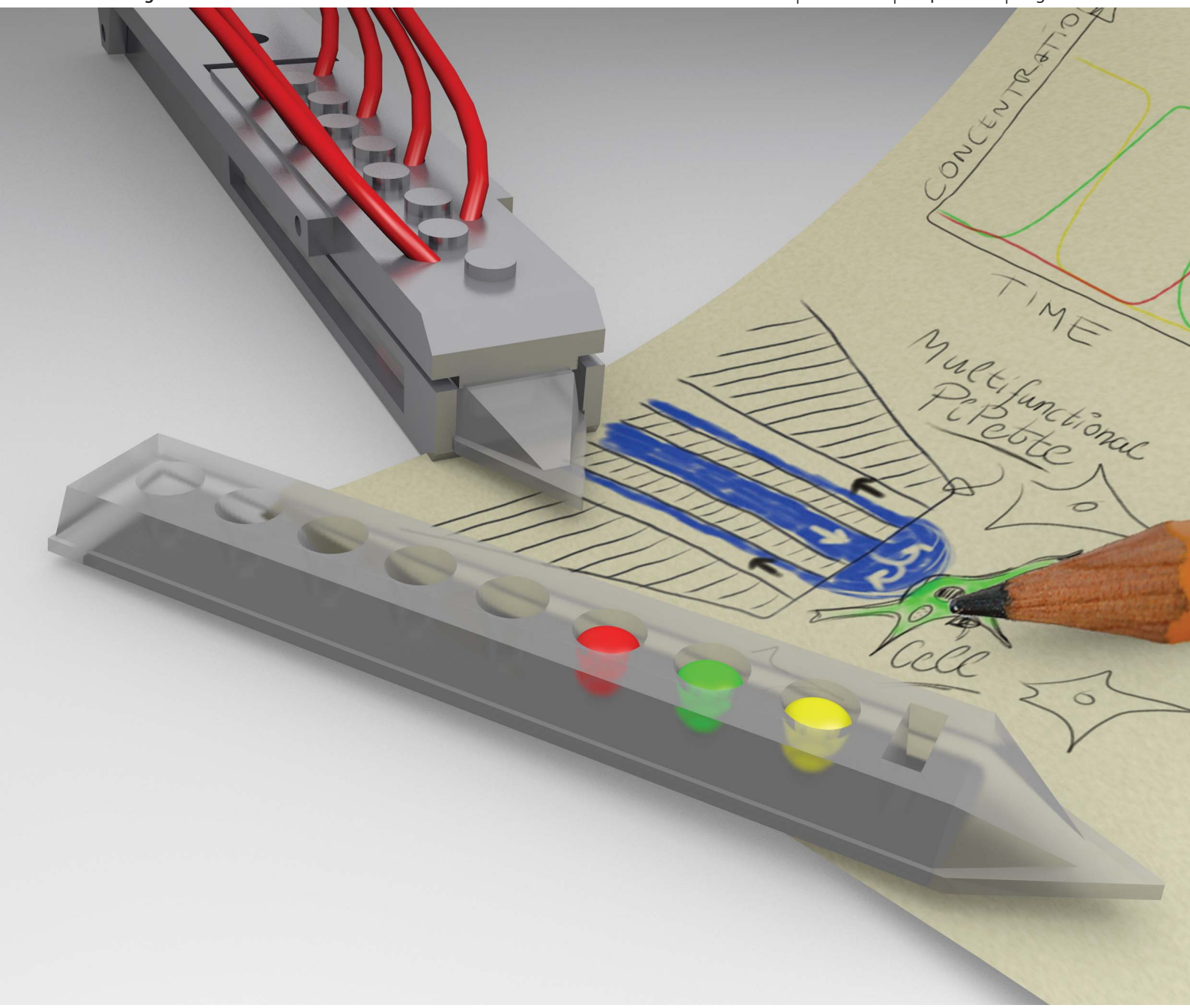

ISSN 1473-0197

RSC Publishing

PAPER

Jesorka *et al.*

A multifunctional pipette

1473-0197(2012)12:7;1-2

Lab on a Chip

Dynamic Article Links

Cite this: *Lab Chip*, 2012, **12**, 1255

www.rsc.org/loc

PAPER

A multifunctional pipette†

Alar Ainla, Gavin D. M. Jeffries, Ralf Brune, Owe Orwar and Aldo Jesorka*

Received 19th September 2011, Accepted 8th December 2011
DOI: 10.1039/c2lc20906c

Microfluidics has emerged as a powerful laboratory toolbox for biologists, allowing manipulation and analysis of processes at a cellular and sub-cellular level, through utilization of microfabricated features at size-scales relevant to that of a single cell. In the majority of microfluidic devices, sample processing and analysis occur within closed microchannels, imposing restrictions on sample preparation and use. We present an optimized non-contact open-volume microfluidic tool to overcome these and other restrictions, through the use of a hydrodynamically confined microflow pipette, serving as a multifunctional solution handling and dispensing tool. The geometries of the tool have been optimised for use in optical microscopy, with integrated solution reservoirs to reduce reagent use, contamination risks and cleaning requirements. Device performance was characterised using both epifluorescence and total internal reflection fluorescence (TIRF) microscopy, resulting in ~200 ms and ~130 ms exchange times at ~100 nm and ~30 μm distances to the surface respectively.

Introduction

Microfluidics has opened a multitude of possibilities for the control of chemical environments at small length scales, enabling functionality and precision which were previously unattainable. The laminar flow regime of microfluidic devices allows the formation and maintenance of spatial concentration gradients,[1] while the introduction of on-chip valves in combination with low dead volumes made possible quick switching between different solutions.[2] To take advantage of this fluidic control using conventional techniques, the sample has to be introduced into the microchannels of the device, which in the context of biological applications is well suited for cell suspensions, but hard to apply when working with adherent cells and tissues.

Recently, several research groups have reported a new class of devices, which can deliver liquid into an open volume while simultaneously rerouting the liquid back into the chip. This is achieved by means of closely spaced adjacent channels under positive and negative pressure, respectively, creating a hydrodynamically confined flow (HCF) volume.[3–5] This volume, fluidically connected to the device tip, can be positioned to stimulate and analyse a single cell or other object of interest, without affecting the surrounding liquid.

Hydrodynamic confinement of one miscible solution inside another is possible due to convective recirculation, counteracting diffusion, which otherwise would mix the two solutions. The balance of convection and diffusion in such an arrangement is described by the dimensionless Péclet number (*Pé*). A larger *Pé* leads to a greater level of confinement, establishing a sharper, more defined boundary between the two liquids.

The idea of recirculation probes originates from physiology, where push–pull cannulae have been used for *in vivo* sampling since 1961.[6] These probes remain popular for sampling of neurotransmitters.[7,8] Hydrodynamic confinement within an open volume was first demonstrated in a picolitre 'fountain-pen' made of two co-axial pipettes, where the inner capillary is used for injection of reagent, and the outer one for aspirating the reagent back into the pipette.[9] Similarly, theta tube capillaries have been applied for recirculation to stimulate cells with lysis buffer and collect the lysate for analysis.[10] Both types of delivery require fragile tips that can be costly and difficult to fabricate.

Later, microfabrication in silicon and polydimethylsiloxane (PDMS) was used to create microfluidic probes, which circulate the liquid in a thin cleft, formed between the face of the probe tip and the surface under investigation.[3,5,11–13] A similar principle has been exploited for use in an electrochemical probe, fabricated from polyethylene terephthalate (PET) and used to analyse dry surfaces.[14] In this case the recirculation provides and refreshes an electrolyte droplet in front of the working electrode. Other free-standing probes have been employed for studying chemotaxis[15] and to deliver genetic material[16] in optical microscopy experiments. The open volume flow recirculation principle has also been applied for stimulating brain slices.[17]

We have previously reported the concept of a HCF microfluidic pipetting device, constructed by sealing channel grooves with a thin membrane.[4] This configuration enables recirculation while allowing for angle adjustment and repositioning of the device. It closely resembles the utility of glass micropipettes, which are typically used in microscopy experiments. This

Department of Chemical and Biological Engineering, Chalmers University of Technology, Kemivägen 10, SE-41296 Göteborg, Sweden. E-mail: aldo@chalmers.se; Fax: +46 31 772 6120; Tel: +46 31 772 6112

† Electronic supplementary information (ESI) available. See DOI: 10.1039/c2lc20906c

particular feature strongly influenced the decision to coin our concept a 'pipette'.

Herein we describe the construction and characterization of a multifunctional pipette, developing the initial concept into a research-ready device, optimized to fit into practically any micromanipulation environment. The pipette has been given a sharp elongated shape, facilitating the application within spatially confined microscopy setups, typically found in bioscience environments, where crowding with probes and manipulation equipment is commonplace. We therefore optimized the geometry to reduce the impact on the microscope sample stage, leaving sufficient space for integrating eight on-chip wells, which can store and provide solutions. We have also created a self-aligning holder, designed for robust clamping of the pipette and providing each well with individual pressure control. The pipette and its interfacing have been optimized for both performance and convenience of use by bioscientists without particular microfluidics expertise.

We provide extensive characterization of the pipette performance, and show exemplary circuitry for on-chip switching between three solutions, which we applied to sequentially deliver capsaicin and calcium to single adherent cells in a surface-adhered collective. The concept is highly flexible, novel circuits and functions can be quickly introduced by using new microstructure molds and adapting the control software accordingly. The holder itself is reusable, allowing for rapid adaptation at low cost.

Methods

Fabrication of the microfluidic tip

Devices (Fig. 1A) were fabricated in PDMS (Dow Corning Sylgard 184) using standard soft-lithography techniques. Instrumental procedures and bonding conditions were applied as previously described.[4] Four pipette tips were simultaneously molded using a polycarbonate form (Hagal Machinery AB, Mölndal, Sweden). To define the pipette shape, reservoir wells and microchannels, a master was fabricated using SU-8 on a 4″ silicon wafer, with characteristics summarized in Table 1. The molded PDMS slab was bonded to a 20 μm thin PDMS film, followed by cutting out each tip and punching out the bottom of the wells. The PDMS part was subsequently bonded to a 0.55 mm thick glass substrate (Praezisions Glas & Optik GmbH, Iserlohn, Germany) to increase the structural strength of the tip and rigidify the body of the device. The step-by-step fabrication procedure is depicted in Fig. S1 of the ESI†.

Holder and control interface

The holder (Fig. 1B) was fabricated in stainless steel (Teadusmosaiik OÜ, Tartu, Estonia) and constitutes a compromise between aqueous solution compatibility, rigidity and cost. The lower part of the holder provides a self-aligning cavity, into which the pipette tips can slide. A cylindrical 7 mm diameter rod is attached at the rear of the holder, to allow for easy interfacing with common micromanipulators.

The upper part of the holder consists of a hinged manifold, which provides pressure connectivity to each of the wells. The underside of this manifold contains sharp flanges (Fig. 1C), which are pushed against the PDMS pipette, sealing it to the manifold when the holder is closed. This interface has been tested to withstand pressures in excess of 2 bar, more than double the maximum operation pressure projected. The manifold connects each well individually with the pressure control unit through a 1 m long and 1 mm I.D. length of Nalgene® PVC tubing, which we determined to be optimal to obtain the fastest pressure switching (see Fig. S2†). Supply pressures were controlled with an in-house developed pressure and valve actuation controller (Fig. S3†), allowing vacuum control within the range 0.00–0.60 ± 0.01 bar, and channel pressure control for two channels in the range between 0.00 and 0.90 ± 0.01 bar (at 95% confidence level). Pressure and vacuum controllers were calibrated with a high precision digital manometer LEX1 (Keller AG, Winterthur, Switzerland). Flow switching is achieved through a valve controller, actuating pressure in the wells with the following specifications: electronic time resolution, 1 ms; delay between the electronic signal and valve opening, 23 ± 2 ms; pressure rise time, 6.0 ± 0.7 ms; delay between the electronic signal and valve closing, 6 ms and pressure fall time, 6 ± 1 ms. All experiments were controlled *via* an in-house programmed graphical user interface, developed in Microsoft Visual Studio 2008.NET (C++).

Characterization

Solution switching within the microfluidic channels and at the pipette outlet was characterized using a 100 μM solution of fluorescein (sodium salt) in deionised water. An inverted microscope Leica DM IRB (Leica Microsystems, Wetzlar, Germany) equipped with a fluorescence lamp, a Leica 10× 0.3 NA air objective, and a Chameleon USB camera (Point Gray Research Inc., Richmond, Canada) was used for experimentation. Alternate visualization was implemented using water soluble food colour in order to highlight the component flows at the switching junction.

Solution switching near the substrate surface (~100 nm) was further characterized using TIRF microscopy with a Leica HCX PL APO 63× 1.67 NA oil TIRF objective, utilising 488 nm Sapphire 488-150 CW CDRH laser excitation (Coherent, Santa Clara, USA).

Cell culturing and stimulation

Adherent Chinese hamster ovary (CHO) cells expressing the human transient receptor potential vanilloid 1 (hTRPV1) ion channel were cultured as previously described.[4] The cells were loaded with calcium sensitive dye, Calcium Green™-1 AM ester (Life Technologies Inc, Carlsbad, USA). At first, a 200 μM stock solution was prepared in DMSO, which was further diluted with Ringer's solution (VWR) to obtain a final concentration of 4 μM. The cells were cultured on Petri dishes equipped with a 0.15 mm thin glass bottom, suitable for confocal imaging. After removing from the incubator, the culture medium was removed and the cells were rinsed twice with Ringer's solution, followed by addition of the dye labelling solution. The cells were exposed to the dye loading solution for 1 h at room temperature, then rinsed twice with Ringer's solution, which was also used as the experimental buffer. 1 μM capsaicin (Sigma-Adrich) and 10 mM, pH 7.4 calcium chloride solution (VWR) were loaded into the multifunctional pipette, and the microscopy experiment was

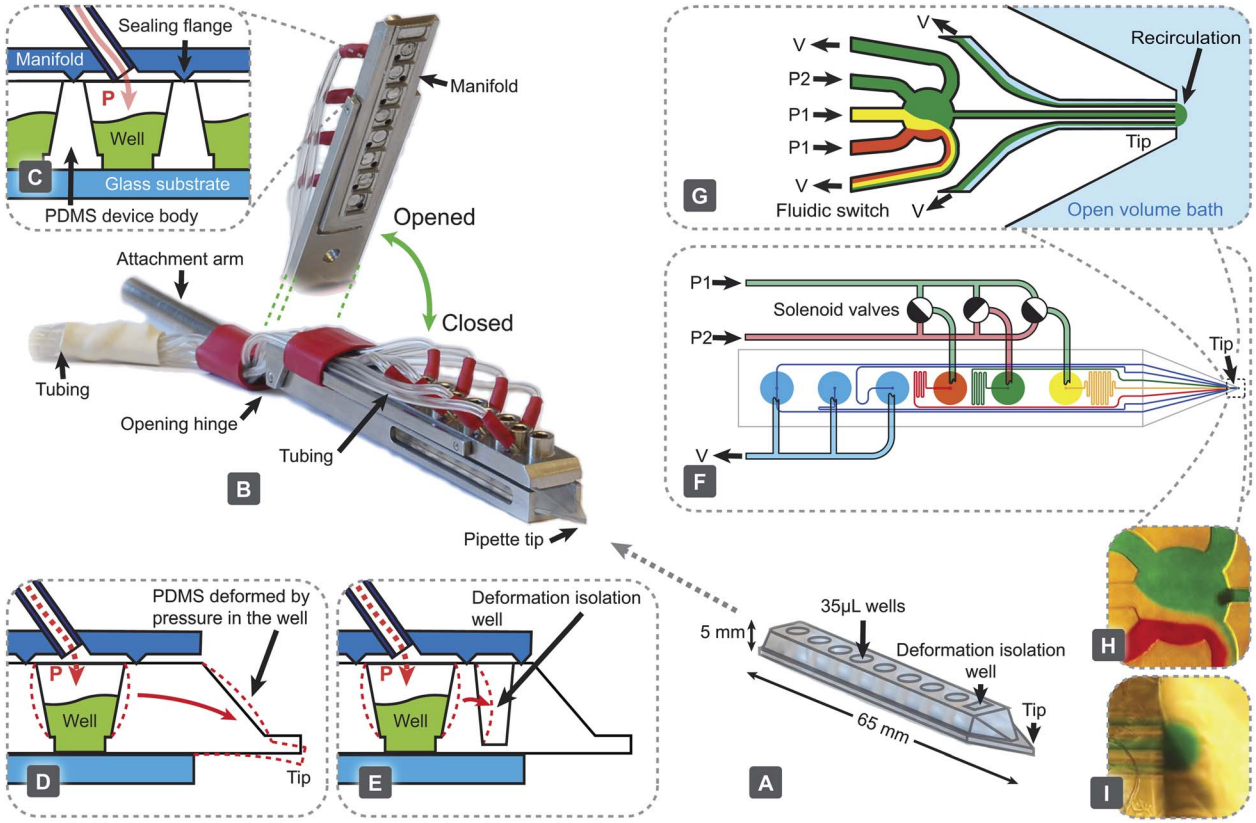

Fig. 1 The multifunctional pipette: components, construction and setup. (A) The PDMS microfluidic pipette tip. (B) The holder, shown in a closed state holding the tip. An elevated angle is also displayed to highlight the manifold's interfacing structure, which contacts the tip. (C) Pneumatic interface between the holder and the tip is formed with sharp flanges protruding from the manifold, which are pushed into the PDMS surrounding the well. Each well has an individual connection, through which pressure can be controlled. (D) Deformation associated with pressure change within the well. (E) Implemented solution to (D), minimising the effects through the use of an isolation well. Exemplary circuitry of a fast 3-solution switch, showing the driving mechanism (F) and the microfluidic switching junction near the tip (G). Microscopy images of a fluidic switching junction (H) and a recirculation volume (I) loaded with coloured water.

performed immediately thereafter. Fluorescence intensity was measured with a Leica DM IRE2 confocal microscope equipped with a Leica TCS SP confocal scanner, an oil-immersion 40× 1.25 NA Leica objective, and Leica Confocal Software (v2.61). Fluorescent intensity was measured from single cells, with excitation at 488 nm and emission collected between 505 and 600 nm.

Simulations

Simulations were performed with COMSOL Multiphysics 4.1, combining models of laminar flow (spf) and transport of dilute species (chds) in stationary and transient 3D models. In the simulations, the mechanical properties used for PDMS were: Young's modulus 1.8 MPa and Poisson's modulus 0.45,[18] the viscosity of water was 1 mPa s and the diffusivity of fluorescein was 5×10^{-10} m^2 s^{-1}.[5]

Results and discussion

Device

In order to demonstrate the multi-functionality of the pipette, we implemented a valveless superfusion device, able to switch between three solutions. Functionally, it is similar to superfusion systems made from glass tubing,[19] but has significantly better reproducibility of geometry and simpler handling. Compared to the valveless switch we have reported previously,[4] the current device does not have dedicated switching channels, removing the

Table 1 Characteristics of microchannels and fluidic circuitry

Characteristic	Symbol	Value	Unit
Channel height	H	20	µm
Channel widths	W	20 and 40	µm
Flow conductance of channels			
Supply/waste/recirculation (well → tip)	G	37	nL s^{-1} bar^{-1}
Outlet (switch → tip)	G_o	500	nL s^{-1} bar^{-1}

restrictions of the resistance of the output channel, connecting the switch to the tip. Switching in our current device occurs when pressures are changed between individually supplied wells (Fig. 1F and G and Movie S1†). A reverse concept has been demonstrated, to sort fractions of a continuous fluid stream, using an inverse flow direction.[20]

Two levels of pneumatic pressure are supplied by the attached pressure control device, and fast switching is achieved through the use of miniature solenoid valves (Fig. S3†). Two pressure levels are needed to avoid backflow from the switch to any of the supply channels, which would cause unwanted mixing of these solutions. For this switching principle to function properly, the pressures applied need to meet certain conditions. The flow rates in the two inactive (switched off) channels have to be smaller than the flow rates to one of the waste channels. In this case only one solution is directed to the output,

$$2G(P_1 - p) < (p + V)G$$

where P_1 denotes the pressure in the solution wells, which are in the "switched off" state, P_2 is the pressure in the wells in the "switched on" state, G and G_0 are the flow conductances as defined in Table 1, V is the vacuum (negative pressure) applied to waste and recirculation wells, and p is the pressure inside the switch junction,

$$p = \frac{G}{5G + G_0}(P_2 + 2P_1 - 2V)$$

Crucially, there must be no backflow from the switch to the wells in the "switched off" state, requiring $p < P_1$. Finally, for typical recirculation settings, the total inflow has to be twice the outflow, requiring $VG \approx pG_0$.

Considering these conditions, and the physical performance limits of our pressure controller, we can derive a set of suitable operation parameters, which are summarized in Table 2. The number of solutions to be switched can be increased, which in the case of our system is limited to seven, as at least one well has to be reserved for recirculation and waste.

Pressure control in elastic devices, such as PDMS, requires attention to possible elastic deformation, which might compromise positioning precision (Fig. 1D). To mitigate motion of the tip during pressure pulsing, we have added a deformation isolation well to the tip and introduced additional flanges toward the front of the manifold (Fig. 1E). These measures reduce unwanted motion during most operations to less than 4 μm in the axial direction (pressure 0.5 bar) (Fig. S4†).

In an attempt to facilitate a more unified design, both the molding tools and the holder have a universal geometry, while the internal circuitry of the pipette tip can be re-designed to address specific experimental needs. This allows very rapid customization, requiring only fabrication of a new channel molding master.

Table 2 Examples of operation settings

Parameter	High flow rate	Medium flow rate	Low flow rate
P_2/bar	0.9	0.5	0.3
P_1/bar	0.2	0.06	0.035
V/bar	0.4	0.19	0.094
Outflow I_0/nL s^{-1}	13.5	6.5	4.9
Run time/min	16	~30	~45 to 120

Solution exchange

Solution exchange performance was characterized using fluorescence microscopy. As epi-fluorescence can only measure the solution exchange within the bulk volume, we combined it with TIRF microscopy, to probe the solution exchange in a confined volume close to the surface of a coverslip, which should provide a better representation of the efficiency of solution exchange around adherent cells than averaging over the recirculation volume. Using high flow rates, the time constant of concentration increase near the surface was found to be 219 ± 94 ms, while concentration decrease was 154 ± 76 ms (Fig. 2), both are sensitive to the positioning of the pipette. The slightly lower fall time can be due to a diffusional dilution effect caused by the surrounding environment, which contains no fluorescent molecules. The solution exchange time in the bulk volume using epi-fluorescence was measured to be ~130 ms.

To elucidate the factors influencing the solution exchange time, we carried out a theoretical evaluation, based on analytical

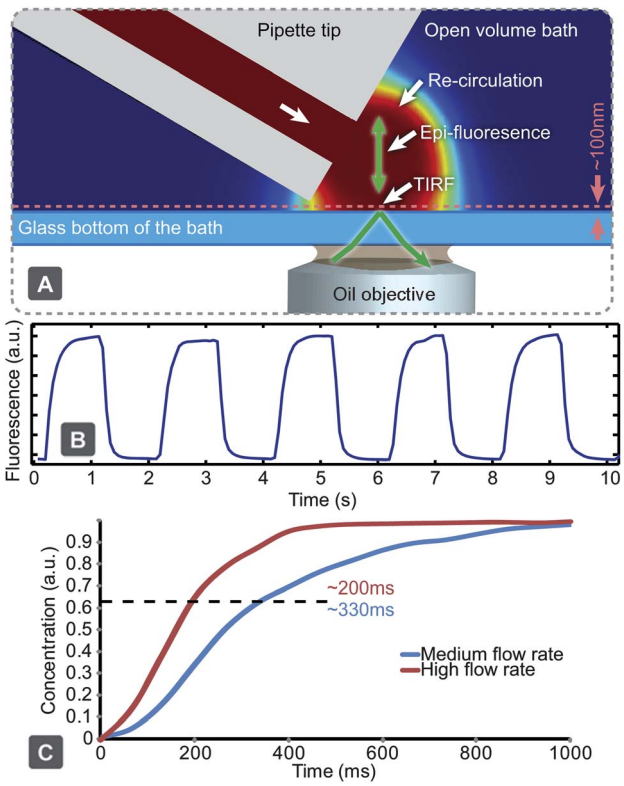

Fig. 2 Characterising solution exchange times. (A) Experimental setup using TIRF microscopy, to monitor solution exchange dynamics near the sample surface. The same setup can be used for epifluorescent measurements of a deeper region, through modification of the excitation angle. (B) Fluorescent intensity measurements of periodic solution exchange near a glass surface using TIRF. (C) Concentration rise time near the surface with high and medium flow rates (~10 and ~5 nL s^{-1}, respectively).

models and finite element simulations (COMSOL). The results are summarized in Table 3, Fig. 3, and in the ESI (Fig. S6–S9†). The largest contribution arose from the flow rate rise time in the supply channel, which is due to the elasticity of PDMS, especially at the end section of the channel, where one of the walls is a thin, unsupported and easily deformable PDMS layer (Fig. S6†). Channel deformability leads to compliance, the hydraulic analogue of capacitance.[21] When coupling this with hydraulic resistance of the channel, a low-pass RC filter is formed, dampening rapid pressure changes, leading to slower flow rate changes towards the end of the channel (Fig. S7†). Thereafter the concentration pulse passes through the outlet channel, where it is subject to dispersion,[22] which broadens the pulse (Fig. S8†).

Once the solution has exited the channel, it has to reach the surface-immobilized cell. Since flow near the surface is restricted due to friction, a short final distance has to be passed mainly by means of diffusion, which occurs at a slower rate (Fig. 3A). Other factors, such as filling the dead volume of the switch, inertia of the liquid and external pressure control, have only minor contributions (Table 3 and Fig. 3B). To improve the switching speed, the outlet channel can be shortened. Enlarging the channel dimensions, which increases the flow rate, would also increase the speed (Fig. S9†). This will reduce the experimental run time as the liquid in the supply wells will be consumed at an accelerated rate. A practical solution in many experiments, since short and long time-scale processes are typically not studied simultaneously, would be to minimize flow rates during setup and positioning ("stand-by mode"), then to only increase supply pressures when high switching speeds are desired. We have implemented such structured modes of operation into the application software. A steeper positioning angle, which would direct the flow closer to the surface, and fabrication in hard materials would be other feasible options to reduce solution exchange times.

The use of a thicker bottom layer for channel sealing can cause opposing effects, reducing, on one hand, the elasticity of the channel, while on the other hand increasing the distance between the channel outlets and surface. Based on simulations and estimations, the exchange speed in this kind of devices could be improved to ~10 to 50 ms (increased flow rates, minimising outlet channel length to the open volume, and use of hard materials for the device). When evaluating fluidic exchange behaviour, it is also necessary to consider the nature of the desired active agent and its diffusivity in solution.

Table 3 Components contributing to the solution exchange time and the dependence of micro-channel geometries l and w, bottom thickness d and flow rate Q (derivations and calculations are supplied in the ESI)

Component	τ/ms	Scaling $\propto$
Solenoid valves	2	
External tubing	4	
Inertia	0.5	$w^2\, l^{-1}$
Supply channel	30	$w^{-1}\, l^2\, d^{-1}$
Dead volume of the switch	2.5	$w^3\, Q^{-1}$
Outlet channel	~70	$w^2\, l^{0.5\ldots\ 1}\, Q^{-0.5\ldots\ -1}$
Outlet to cell	~40	
Sum	~150	

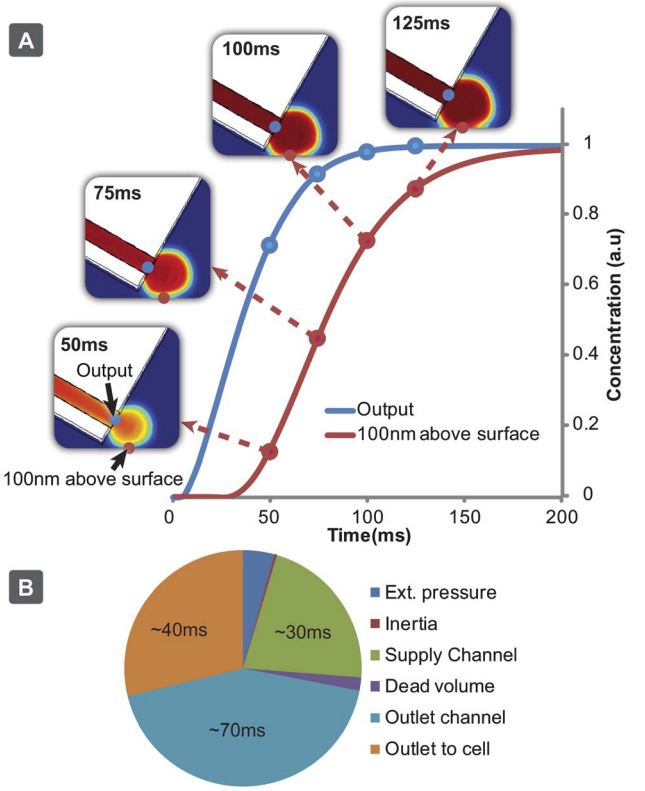

Fig. 3 Results of a computer simulation to model the fluidic exchange times close to the sample surface. (A) Concentration rise time near the surface (100 nm above) and at the channel output. (B) Contributing factors and influence to the solution exchange time, based on experimental results, simulations and calculations.

Application to single cell studies

Delivery of stimuli to individual cells allows for exquisite analysis of cellular function while enabling the mapping of population heterogeneity. However, greater levels of detail can be extracted by simultaneous exposure of small collectives of cells, where individual cell analysis can be made on their response. The multifunctional pipette offers a flexible way to address either situation, through control of recirculation flow and positioning (Fig.S5 and Movie S2†).

An adherent CHO cell culture, expressing hTRPV1, was used to demonstrate the use of the device for chemical stimulation of single cells, through the sequential delivery of active compounds to selected cells from within a collective. The cells were pre-treated with a cell-penetrating, mildly fluorescent species, which upon entering the cell is enzymatically converted into a calcium chelator. In the presence of calcium ions this molecule forms a highly fluorescent complex, which can be readily detected. Using the multifunctional pipette, the dye loaded cells were first treated with a 10 s pulse of capsaicin to activate the hTRPV1 channel, then washed for 5 s and treated with a 10 s pulse of Ca^{2+}. After 50 s, the Ca^{2+} pulse was repeated. Cells that had been exposed to capsaicin became Ca^{2+} permeable, which was observed by their rapid increase in fluorescent intensity, whereas Ca^{2+} applied to cells not treated with capsaicin demonstrated no significant increase. A slight shape change was observed during

the course of the experiment, likely due to a slight osmotic pressure imbalance.

Interestingly, we observed several different types of cellular response, as depicted in Fig. 4C. Some cells exhibited a strong response to the first calcium pulse, but not to the second (Cell 1), while others responded to both pulses (Cell 2). Varied loading efficiencies of the indicator dye within the cell population gave a wide range of initial fluorescence intensity values. One such cell was selected from the background population outside the recirculation zone (Cell 3) and demonstrated no response to the calcium pulses, indicating fluidic isolation from the targeted cells. The observed variable calcium responses may be cell population heterogeneity, or flow velocity dependent, as lateral positioning with respect to the pipette tip will determine the flow rate. Some cells situated within the centre of the recirculation zone (marked with a dashed line) exhibited behaviour similar to an internal calcium release. Capsaicin application and high flow velocities within this region may have contributed to this type of cellular response.

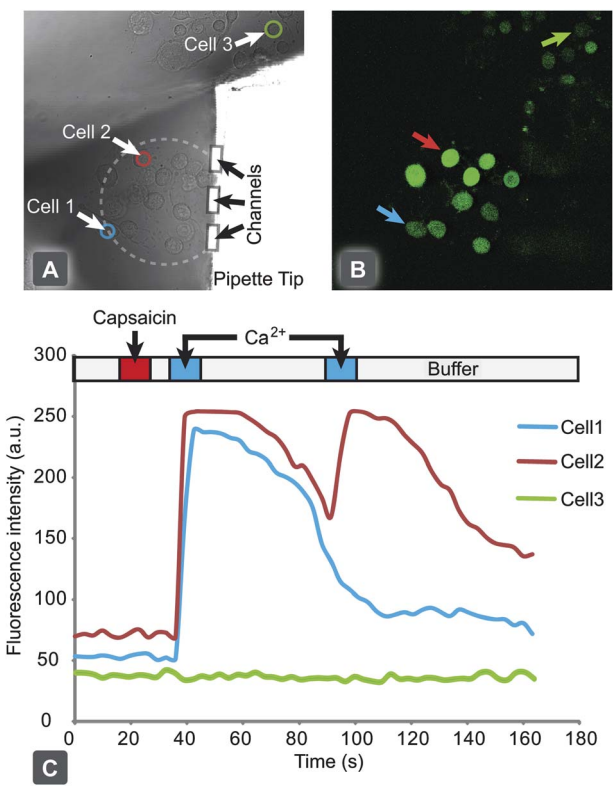

Fig. 4 Chemical stimulation and response of individual *h*TRPV1 expressing CHO cells, through activation with capsaicin. (A) Bright field microscopy image of adherent cell culture of *h*TRPV1 expressing CHO cells, with the pipette tip targeting a small collective. (B) Confocal fluorescent micrograph of Calcium Green™ loaded cells after stimulation with capsaicin and subsequent exposure to Ringer's solution, spiked with 10 mM calcium chloride. (C) A graph of individual cellular responses to the application protocol, with the delivery times highlighted above. Cells 1 and 2 are within the recirculation zone and display a positive activation response. Cell 3 is a representative cell from the background outside of the stimulation zone.

Conclusion

We have created a free-standing multifunctional pipette for highly localized perfusion in single cell experiments. It addresses the needs for facile setup, handling, and application. The pipette was developed from an HCF principle, enabling contamination-free confinement of one miscible liquid inside another. Molding in PDMS allows pipette fabrication at low cost and high flexibility, as compared to microfluidic probes made of hard materials,[3,11] where fabrication requires complex processing equipment such as a mask-aligner, deep reactive ion etching (DRIE), bonder, polishing tools and also a cleanroom environment. Soft-lithography requires only a photolithographically fabricated master, which can be re-used for many cycles, a spin-coater, and an inspection microscope. A plasma chamber was used for bonding our device together, which provides better reproducibility than other attachment techniques. An additional benefit of molded devices is that solution wells can be easily integrated into the same component piece. Apart from easy handling and lower reagent consumption, the use of integrated wells completely overcomes the typical problem of the dead volume of external tubing, which is usually significantly larger than the volume of the microchannels. A major benefit in comparison to other microfluidic HCF devices is the possibility to approach the recirculation volume with other probes, such as patch pipettes, optical fibres, or electrodes. It can be used together with upright microscopes at lower application angles, as the sharp tip produces minimal optical disturbance (shadowing) of a transmission image, which can be minimised using oblique and/or ring illumination.

We have also demonstrated that the internal fluid processing circuitry can be contained within a recirculation device, minimizing on-chip dead volumes and decreasing the solution switching times. Hard material microfluidic probes could offer advantages when very small recirculation volumes are desired, since vertical configuration and circulation in small clefts allow for forcing liquid circulation closer to the surface and to achieve higher Péclet numbers. This is mostly favourable for chemical surface processing, but less applicable for cell cultures and tissue, as high shear stress can move, detach and destroy cellular structures. Moving away from elastomeric materials would also remove device compliance, which will allow faster solution switching.

In summary, we believe that the versatility, simplicity of design, and ease of integration of the multifunctional pipette, either as a primary or supporting device, will impact single cell and tissue culture research, most prominently in neuroscience and pharmacology, where it can amend current superfusion techniques and open new application areas.

Acknowledgements

This research was funded by the European Research Council (ERC grant), Swedish Research Council (VR), the Knut and Alice Wallenberg Foundation, the Swedish Strategic Research Foundation (SSF), and the National Institute of Health (NIH). We thank AstraZeneca R&D CNS&P Södertälje for the cell line stably expressing the human TRPV1 ion channel and Erik T. Jansson and Carolina Boström for maintenance of the cell line.

Notes and references

1 S. K. W. Dertinger, D. T. Chiu, N. L. Jeon and G. M. Whitesides, *Anal. Chem.*, 2001, **73**, 1240–1246.
2 M. A. Unger, H. P. Chou, T. Thorsen, A. Scherer and S. R. Quake, *Science*, 2000, **288**, 113–116.
3 D. Juncker, H. Schmid and E. Delamarche, *Nat. Mater.*, 2005, **4**, 622–628.
4 A. Ainla, E. T. Jansson, N. Stepanyants, O. Orwar and A. Jesorka, *Anal. Chem.*, 2010, **82**, 4529–4536.
5 K. V. Christ and K. T. Turner, *Lab Chip*, 2011, **11**, 1491–1501.
6 J. H. Gaddum, *J. Physiol.*, 1961, **155**, P1.
7 S. Kottegoda, I. Shaik and S. A. Shippy, *J. Neurosci. Methods*, 2002, **121**, 93–101.
8 N. A. Cellar, S. T. Burns, J. C. Meiners, H. Chen and R. T. Kennedy, *Anal. Chem.*, 2005, **77**, 7067–7073.
9 O. Feinerman and E. Moses, *J. Neurosci. Methods*, 2003, **127**, 75–84.
10 H. Shiku, T. Yamakawa, Y. Nashimoto, Y. Takahashi, Y.-s. Torisawa, T. Yasukawa, T. Ito-Sasaki, M. Yokoo, H. Abe, H. Kambara and T. Matsue, *Anal. Biochem.*, 2009, **385**, 138–142.
11 G. V. Kaigala, R. D. Lovchik, U. Drechsler and E. Delamarche, *Langmuir*, 2011, **27**, 5686–5693.
12 R. D. Lovchik, U. Drechsler and E. Delamarche, *J. Micromech. Microeng.*, 2009, **19**, 115006.
13 A. Queval, N. R. Ghattamaneni, C. M. Perrault, R. Gill, M. Mirzaei, R. A. McKinney and D. Juncker, *Lab Chip*, 2009, **10**, 326–334.
14 D. Momotenko, F. Cortes-Salazar, A. Lesch, G. Wittstock and H. H. Girault, *Anal. Chem.*, 2011, **83**, 5275–5282.
15 W. K. Raja, B. Gligorijevic, J. Wyckoff, J. S. Condeelis and J. Castracane, *Integr. Biol.*, 2010, **2**, 696–706.
16 H. Tavana, A. Jovic, B. Mosadegh, Q. Y. Lee, X. Liu, K. E. Luker, G. D. Luker, S. J. Weiss and S. Takayama, *Nat. Mater.*, 2009, **8**, 736–741.
17 Y. T. Tang, J. Kim, H. E. Lopez-Valdes, K. C. Brennan and Y. S. Ju, *Lab Chip*, 2011, **11**, 2247–2254.
18 F. Schneider, T. Fellner, J. Wilde and U. Wallrabe, *J. Micromech. Microeng.*, 2008, 18.
19 N. S. Veselovsky, F. Engert and H. D. Lux, *Pfluegers Arch.*, 1996, **432**, 351–354.
20 C. A. Baker and M. G. Roper, *J. Chromatogr., A*, 2010, **1217**, 4743–4748.
21 H. Bruus, *Theoretical Microfluidics*, Oxford University Press, 2007.
22 *Physiochemical Hydrodynamics*, ed. R. F. Probstein, John Wiley & Sons, 1995.